Eur. Phys. J. A (2016) **52**: 257
DOI 10.1140/epja/i2016-16257-0

THE EUROPEAN PHYSICAL JOURNAL A

Review

Thermal electromagnetic radiation in heavy-ion collisions*

R. Rapp[1] and H. van Hees[2,3,a]

[1] Cyclotron Institute and Department of Physics & Astronomy, Texas A&M University, College Station, TX 77843-3366, USA
[2] Institut für Theoretische Physik, Goethe-Universität Frankfurt, Max-von-Laue-Str. 1, D-60438 Frankfurt, Germany
[3] Frankfurt Institute of Advanced Studies (FIAS), Ruth-Moufang-Str. 1, D-60438 Frankfurt, Germany

Received: 10 December 2015 / Revised: 12 February 2016
Published online: 24 August 2016 – © Società Italiana di Fisica / Springer-Verlag 2016
Communicated by D. Blaschke

Abstract. We review the potential of precise measurements of electromagnetic probes in relativistic heavy-ion collisions for the theoretical understanding of strongly interacting matter. The penetrating nature of photons and dileptons implies that they can carry undistorted information about the hot and dense regions of the fireballs formed in these reactions and thus provide a unique opportunity to measure the electromagnetic spectral function of QCD matter as a function of both invariant mass and momentum. In particular we report on recent progress on how the medium modifications of the (dominant) isovector part of the vector current correlator (ρ channel) can shed light on the mechanism of chiral symmetry restoration in the hot and/or dense environment. In addition, thermal dilepton radiation enables novel access to a) the fireball lifetime through the dilepton yield in the low invariant-mass window $0.3\,\mathrm{GeV} \leq M \leq 0.7\,\mathrm{GeV}$, and b) the early temperatures of the fireball through the slope of the invariant-mass spectrum in the intermediate-mass region ($1.5\,\mathrm{GeV} < M < 2.5\,\mathrm{GeV}$). The investigation of the pertinent excitation function suggests that the beam energies provided by the NICA and FAIR projects are in a promising range for a potential discovery of the onset of a first-order phase transition, as signaled by a non-monotonous behavior of both low-mass yields and temperature slopes.

1 Introduction

Photons and dileptons have long been recognized as valuable probes of the hot and dense medium created in heavy-ion collisions (HICs). Since they can leave the reaction zone essentially unaffected by final-state interactions, they mediate direct information on the properties of the partonic and hadronic electromagnetic (EM) current-current correlation function in the system in both time-like (dileptons) and light-like (photons) domains. The thermal emission rates can be concisely written in terms of the (retarded) spectral function of the EM current-correlation function in the medium, $\rho_{\mathrm{em}} = -\,\mathrm{Im}\,\Pi_{\mathrm{em}}/\pi$, as [1,2]

$$\frac{\mathrm{d}N_{\ell\ell}}{\mathrm{d}^4x\mathrm{d}^4q} = -\frac{\alpha_{\mathrm{em}}^2}{\pi^3 M^2} f_{\mathrm{B}}(q_0;T) \times \frac{1}{3} g_{\mu\nu}\,\mathrm{Im}\,\Pi_{\mathrm{em,ret}}^{\mu\nu}(M,q;T,\mu_B), \quad (1)$$

$$q_0\frac{\mathrm{d}N_{\gamma}}{\mathrm{d}^4x\mathrm{d}^3\boldsymbol{q}} = -\frac{\alpha_{\mathrm{em}}}{\pi^2} f_{\mathrm{B}}(q_0;T) \times \frac{1}{2} g_{\mu\nu}\,\mathrm{Im}\,\Pi_{\mathrm{em,ret}}^{\mu\nu}(M=0,q;T,\mu_B), \quad (2)$$

where f_{B} denotes the thermal Bose distribution function and $\alpha_{\mathrm{em}} \simeq 1/137$ the EM coupling constant (T: temperature, μ_B: baryon chemical potential; q^0 and q are the energy and momentum of the dilepton or photon in the (local) rest frame of the medium). The key difference between the two expressions is that the dilepton rate, eq. (1), depends on the invariant mass, $M^2 = q_0^2 - q^2$, of the virtual photon, while the photon rate, eq. (2), constitutes the $M \to 0$ limit and thus only depends on the photon's three-momentum (or energy), $q_0 = q$. The rate expressions are remarkably simple, as a product of a thermal distribution function and the EM spectral function of the medium. Dilepton spectra are the only known observables in HICs which provide direct access to a spectral function of the QCD medium. This encodes a rich physics potential that will be further elaborated below. In practice, the measured spectra contain contributions from all stages of the evolution of a HIC, requiring realistic bulk evolution models over which the rates need to be integrated over.

The EM spectral function is well known in vacuum from the inverse process of $\mathrm{e}^+\mathrm{e}^-$ annihilating into hadrons, cf. fig. 1. It simply represents the excitation spectrum of the QCD vacuum in the vector channel, $J^P = 1^-$, *i.e.*, for the quantum numbers of the photon. For masses relevant for thermal radiation in HICs, $M \lesssim 3\,\mathrm{GeV}$, it exhibits two basic regimes. In the low-mass region, $M \lesssim 1\,\mathrm{GeV}$,

* Contribution to the Topical Issue "Exploring strongly interacting matter at high densities - NICA White Paper" edited by David Blaschke *et al.*

[a] e-mail: hees@fias.uni-frankfurt.de

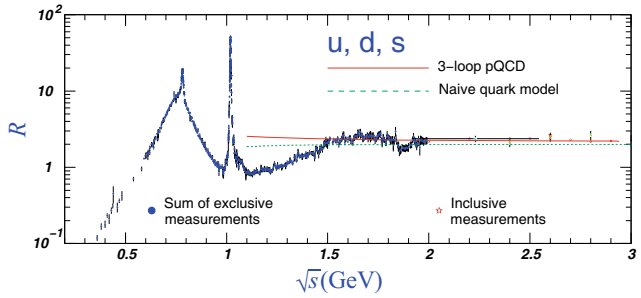

Fig. 1. Cross section ratio for $e^+e^- \to$ hadrons to $e^+e^- \to \mu^+\mu^-$, which is directly proportional to the vacuum EM spectral function, $R = 12\pi^2\rho_{\rm em}/M^2$. Figure redrawn from ref. [3].

the strength is concentrated in the light vector meson peaks corresponding to ρ, ω, and ϕ. In the intermediate-mass region, $1.5\,\text{GeV} \lesssim M \lesssim 3\,\text{GeV}$, the strength of the hadronic spectrum is essentially given by the perturbative $q\bar{q}$ continuum (subsequent hadronization does not significantly affect the short distance processes determining the cross section). The vacuum EM spectral function therefore exhibits a clean transition from confined hadronic degrees of freedom to weakly interacting quarks and antiquarks as the resolution ($q^2 = M^2$) of the probe is increased. In particular, the low-mass part clearly signals the non-perturbative physics of the QCD vacuum related to its quark and gluon condensate structures. By measuring dilepton spectra in HICs one essentially puts this probe into the QCD medium. This suggests that low-mass spectra can monitor the fate of hadrons as temperature and density are increased and thus reveal underlying changes in the condensates, often referred to as chiral symmetry restoration associated with the melting of the quark-antiquark condensate, $\langle\bar{q}q\rangle$. As will be discussed below, most of the low-mass radiation in high-energy HICs indeed emanates from temperatures around the pseudo-critical chiral transition temperature, $T_{\rm pc}^{\chi} \simeq 155\,\text{MeV}$ [4,5], rendering low-mass dileptons an excellent observable to investigate this transition. On the other hand, for masses above $M \simeq 1.5\,\text{GeV}$, temperature corrections to the EM spectral function are small (of order $\mathcal{O}(T^2/M^2)$), and dilepton spectra become an excellent thermometer of the produced medium. As is well known [6,7], large invariant masses exponentially favor the emission of early (hot) radiation, dominating over the volume increase which grows with a power (typically 5-6) in T. While the temperature slope of the invariant-mass spectra involves a certain average over a range of fireball temperatures, it is not distorted by any ("Doppler") blue shift due to the radial flow of the expanding medium (invariant-mass distributions do not change under Lorentz boosts). This is different for momentum spectra of thermal photons (or dileptons), where an expanding medium imparts a significant blue shift on the spectra which has to be deconvoluted before a "true" temperature can be extracted [8].

In the remainder of this contribution, we first briefly review the relevance of chiral symmetry, its breaking and restoration in the context of dileptons and then discuss recent work pertinent to it (sect. 2). We present the current state of phenomenology of EM radiation in HICs and offer perspectives for the energy regime covered by NICA (sect. 3), followed by concluding remarks (sect. 4).

2 Chiral symmetry and dileptons

The QCD Lagrangian

$$\mathscr{L}_{\rm QCD} = \bar{q}(\mathrm{i}\not{\mathrm{D}} - \hat{m}_q)q - \frac{1}{4}G^a_{\mu\nu}G^{\mu\nu}_a,$$
$$\text{with} \quad \mathrm{D}_\mu = \partial_\mu + \mathrm{i}g\frac{\lambda_a}{2}A^a_\mu, \tag{3}$$

is formulated in terms of quark fields q carrying both color and flavor indices with a diagonal current-quark mass matrix $\hat{m}_q = \text{diag}(m_u, m_d, m_s, \ldots)$. The gluon fields A^a_μ are contracted with the 8 Gell-Mann matrices λ_a acting in SU(3) color space, with a non-Abelian field-strength tensor $G^a_{\mu\nu} = \partial_\mu A^a_\nu - \partial_\nu A^a_\mu - g f^{abc} A^b_\mu A^c_\nu$, where the f^{abc} are the SU(3) structure constants. The chiral symmetry of $\mathscr{L}_{\rm QCD}$ refers to its approximate invariance under the spin-isospin rotations in the u and d sector,

$$q \to \exp(-\mathrm{i}\boldsymbol{\alpha}_{\rm V}\cdot\boldsymbol{\tau}/2)q$$
$$\text{and} \quad q \to \exp(-\mathrm{i}\gamma_5\boldsymbol{\alpha}_{\rm A}\cdot\boldsymbol{\tau}/2)q, \tag{4}$$

where $\boldsymbol{\tau}$ are the SU(2) isospin matrices. This symmetry is explicitly broken by small light quark masses, $m_{u,d} \ll \Lambda_{\rm QCD}$ (which can be treated as a perturbation giving rise to "chiral perturbation theory" as a low-energy effective theory of QCD). Chiral symmetry leads to (partially) conserved isovector-vector and -axialvector currents,

$$\boldsymbol{j}^\mu_V = \bar{q}\gamma^\mu\frac{\boldsymbol{\tau}}{2}q, \qquad \boldsymbol{j}_A = \bar{q}\gamma^\mu\gamma_5\frac{\boldsymbol{\tau}}{2}q, \tag{5}$$

also referred to as a chiral multiplet, usually associated with the lowest-lying resonances $\rho(770)$ and $a_1(1260)$ in each channel. Other chiral multiplets are identified as, *e.g.*, $\sigma(500)$-$\pi(140)$, $N(940)$-$N^*(1535)$. The large splitting of the chiral multiplets is commonly attributed to the spontaneous breaking of chiral symmetry in the vacuum, $\text{SU(2)}_{\rm L} \times \text{SU(2)}_{\rm R} \to \text{SU(2)}_{\rm V}$, induced by the formation of the quark condensate, $\langle\bar{q}q\rangle \simeq 2\,\text{fm}^{-3}$ per quark flavor, where pions arise as the pseudo-Goldstone modes of the unbroken directions of the global symmetry.

As discussed above, the low-mass part of the EM spectral function is well described by the spectral functions of the light vector mesons,

$$\rho_{\rm em} = -\frac{1}{\pi}\,\text{Im}\left[\frac{m_\rho^4}{g_\rho^2}D_\rho + \frac{m_\omega^4}{g_\omega^2}D_\omega + \frac{m_\phi^4}{g_\phi^2}D_\phi\right], \tag{6}$$

known as the vector-meson dominance (VMD) [9,10] hypothesis, which arises from the current-field identity $j^\mu_V = (m_V^2/g_V)V^\mu$ ($V \in \{\rho,\omega,\phi\}$). Since the contributions to $\rho_{\rm em}$ are dominated by the ρ meson, calculations of medium effects have focused on the latter. Hadronic many-body

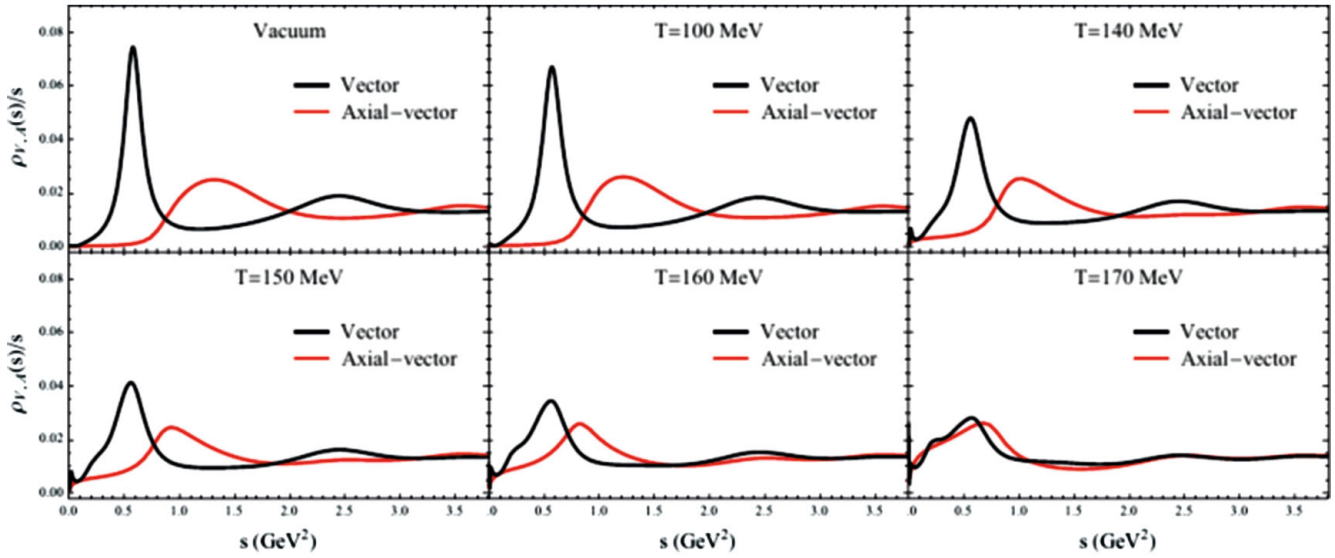

Fig. 2. Temperature progression (at $\mu_B = 0$) of the axialvector spectral function (red lines) as inferred from a simultaneous solution of QCD and Weinberg sum rules [11] using as input an in-medium vector spectral function from hadronic many-body theory [12] (black lines) and in-medium condensates as available from lattice QCD.

approaches generically find a strong broadening of the ρ-meson spectral function in hot/dense matter, leading to a melting of its resonance structure mostly driven by interactions with baryons and anti-baryons [13]. These approaches lead to a good description of all available dilepton data in HICs (see sect. 3 below). A rigorous relation of the ρ melting to chiral restoration has not been established yet, but progress has been made recently.

In ref. [11], a combined analysis of finite-temperature QCD [14] and Weinberg [15] sum rules has been carried out to test the in-medium ρ spectral function that describes dilepton spectra [12] with respect to chiral restoration. QCD sum rules relate power series with quark and gluon condensates to spectral functions for a given quantum number, while Weinberg sum rules specifically relate moments of the difference between isovector-vector (ρ) and -axialvector (a_1) spectral functions to chiral order parameters (pion decay constant, quark condensate, etc.). Using the latter as input from lattice-QCD (augmented by hadron resonance gas predictions where needed) together with calculated in-medium ρ spectral functions, viable in-medium a_1 spectral functions were searched for that can satisfy both QCD and Weinberg sum rules within their typical accuracy of $\sim 0.5\%$. A solution was found that gradually degenerates with the vector-meson spectral function, cf. fig. 2. This implies that our current understanding of dilepton data is compatible with (the approach toward) chiral symmetry restoration. This analysis also suggests a mechanism of chiral restoration by which the broadening of both ρ and a_1 is accompanied by a reduction of the a_1 mass moving toward the ρ mass, while the latter approximately stays constant. A microscopic investigation of the in-medium π-ρ-a_1 system has recently been conducted within the Massive-Yang Mills (MYM) framework [16]. First, the notorious difficulties of the MYM approach to describe the vacuum axialvector spectral function could be overcome by introducing a broad ρ propagator into the a_1 self-energy, accompanied by judiciously chosen vertex corrections to maintain PCAC [17]. A one-loop finite-T calculation results in a moderate broadening of both peaks, as well as a downward mass shift of the a_1 by up to about 200 MeV along with a 15–20% reduction of the pion decay constant and scalar condensate. This result is remarkably similar to the phenomenological sum rule analysis and corroborates the "burning" of the chiral mass splitting as a mechanism of restoring chiral degeneracy. The extension of this analysis to finite baryon densities remains a formidable task. Finally, a recent lattice-QCD calculation has investigated the behavior of the nucleon correlation function and its chiral partner, $N^*(1535)$, at finite T [18]. Also here it was found that the mass of the ground state (nucleon) remains essentially stable while the mass of the excited state approaches the former and degenerates with it around $T_{\rm pc}$.

3 Dilepton production in heavy-ion collisions

Large efforts have been devoted over the past decades to calculate photon and dilepton spectra in HICs in comparison to experimental data. For low-mass dilepton spectra, a consistent picture has emerged in terms of a broadening ρ spectral function in the hadronic phase which smoothly merges into a quark-antiquark continuum in the QGP around temperatures of $T_{\rm pc} \simeq 170$ MeV. When implemented into an expanding thermal fireball which utilizes a modern lattice-QCD based equation of state (EoS) and is tuned to fit hadronic yields and spectra, the high-precision NA60 data [19] in In-In collisions (as well as NA45/CERES data [20,21] in Pb-Au collisions) at CERN-SPS energies ($\sqrt{s} = 17.3$ GeV) are well described; pertinent predictions for the excitation function in Au-Au collisions for $\sqrt{s} = 19.6$, 27, 39, 62.4 and 200 GeV

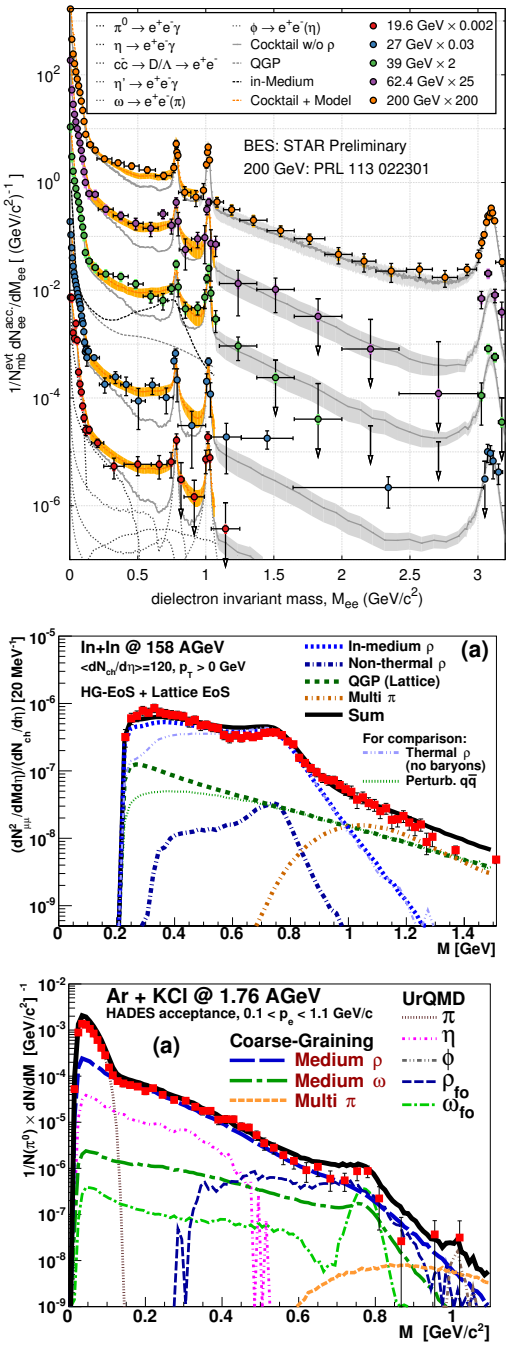

Fig. 3. Dilepton invariant-mass spectra from SIS-18 to top RHIC energies using the in-medium ρ spectral function of ref. [12] for hadronic emission and in-medium $q\bar{q}$ annihilation from the QGP. Top panel: excitation function measured in Au-Au collisions by STAR [22,23], compared to predictions using a thermal fireball model [24]. (Figure reprinted with permission from [22].) Lower two panels: NA60 data in In-In at CERN-SPS (middle panel) and Ar-KCl at GSI-SIS-18 (lower panel) calculated with the same dilepton emission rates implemented into a coarse-grained UrQMD approach [25,26].

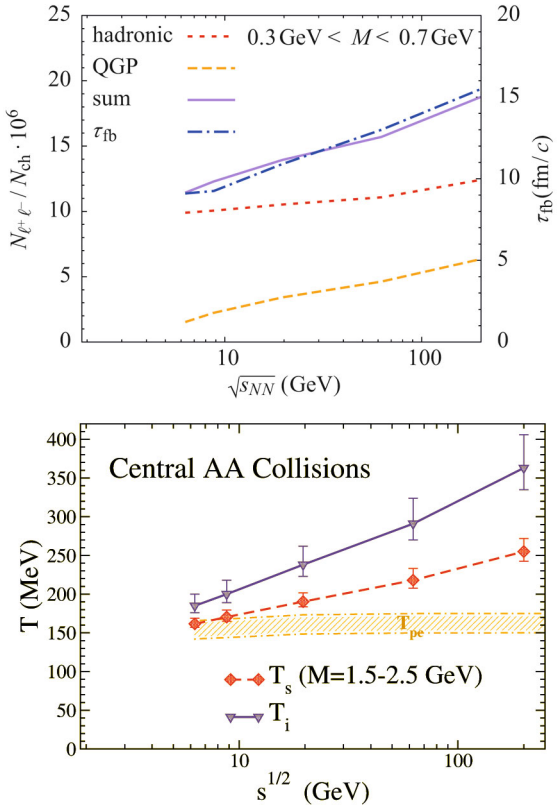

Fig. 4. Excitation function of thermal dilepton radiation in central HICs. Upper panel: The integrated dilepton yield in the mass range $0.3\,\mathrm{GeV} \leq M_{\mathrm{ee}} \leq 0.7\,\mathrm{GeV}$, serving as fireball chronometer; lower panel: The inverse slope parameter over the invariant-mass range $1.5\,\mathrm{GeV} \leq M_{\mathrm{ee}} \leq 2.5\,\mathrm{GeV}$, serving as fireball thermometer. Figures taken from ref. [28].

agree with the STAR data [22,23], cf. upper panel in fig. 3. Notably, the large enhancement reported earlier by PHENIX [27] has recently been revisited: their most recent data [29] are now consistent with the STAR data and theory predictions. At lower energies, larger initial overlap times of the colliding nuclei as well as prolonged thermalization times may render bulk evolution models based on rapid local equilibration (fireball and/or hydrodynamics) problematic. In order to still utilize the conceptually sound concept of thermal EM emission rates, a coarse-graining approach of a realistic bulk medium evolution has recently been implemented [26,25]: well-tested UrQMD transport simulations are averaged over many events on a space-time grid, where the local baryon densities and p_t spectra are mapped to a hadron resonance gas EoS for $T \leq T_{\mathrm{pc}}$ and a lattice-QCD based EoS above. Using the same dilepton rates as in the fireball calculations, the NA60 data are reproduced with similar quality as in the fireball model [25], cf. middle panel of fig. 3. Running the same approach at the much lower energies of SIS-18 at GSI, the HADES data are remarkably well reproduced without free parameters, cf. lower panel of fig. 3.

The robust understanding of all existing low-mass dilepton spectra allows to take this observable to the next level, by exploiting it as a probe of fundamental fireball properties across the QCD phase diagram. In ref. [28] this has been put forward in two respects, by extracting a) the total fireball lifetime from the excess yields in

the low-mass region, and b) the early fireball temperatures from the invariant-mass slopes in the intermediate-mass region. The results for central AA collisions (with atomic number $A \simeq 200$) in the ultrarelativistic energy regime, $\sqrt{s} > 6\,\mathrm{GeV}$, are summarized in fig. 4. The upper panel shows that the thermal dilepton yield in the mass range $0.3\,\mathrm{GeV} \leq M_{\mathrm{ee}} \leq 0.7\,\mathrm{GeV}$ is an excellent measure of the total lifetime of the fireball (other mass regions, *e.g.*, around the free ρ mass do not work as well); this could become particularly useful if lifetime variations occur due to a softening of the EoS, possibly resulting in a non-monotonous energy dependence. The lower panel shows that the slope of the spectrum extracted over the range $1.5\,\mathrm{GeV} \leq M_{\mathrm{ee}} \leq 2.5\,\mathrm{GeV}$ is a direct measure of the temperature in the early phases of the fireball evolution, well inside the QGP at top-SPS energy and beyond, but reflecting and tracing the mixed phase for $\sqrt{s} \lesssim 10\,\mathrm{GeV}$. A possible plateau toward lower energies, before dropping to the lower temperatures of the SIS-18 regime, would be a rather strong evidence for the onset of a mixed phase and thus the discovery of a first-order transition.

4 Conclusions

Dileptons remain a prime probe of the interior medium of the fireballs produced in HICs. A robust understanding of existing data has emerged over the last decade, in terms of a melting of the ρ meson as the phase boundary is approached from below. This is indicative of a change from hadronic to partonic degrees of freedom and compatible with the restoration of the spontaneously broken chiral symmetry. While the precise mechanism for the restoration remains to be determined, current theoretical models suggest the degeneracy of chiral multiplets to be realized by burning off the chiral mass splitting in the vacuum with the ground state mass being stable. We have shown how thermal dilepton radiation can be taken to the next level as a probe of fundamental fireball properties such as its total lifetime and early temperatures. A particularly promising regime for the pertinent excitation functions turns out to be collision energies of $\sqrt{s} \simeq 2$–$8\,\mathrm{GeV}$. Since this regime is uncharted territory in terms of low-mass dilepton measurements with heavy ions to date, its exploration at the future NICA facility is a compelling case. The situation might become a bit more involved if novel spectral structures emerge in the vector spectral function close to the putative critical point. However, this rather provides an additional potential for new discoveries.

This work has been supported by the US-NSF under grant No. PHY-1306359.

References

1. L.D. McLerran, T. Toimela, Phys. Rev. D **31**, 545 (1985).
2. C. Gale, J.I. Kapusta, Nucl. Phys. B **357**, 65 (1991).
3. Particle Data Group (K. Nakamura *et al.*), J. Phys. G **37**, 075021 (2010).
4. Y. Aoki, Z. Fodor, S.D. Katz, K.K. Szabo, Phys. Lett. B **643**, 46 (2006).
5. T. Bhattacharya *et al.*, Phys. Rev. Lett. **113**, 082001 (2014).
6. E.V. Shuryak, Phys. Rep. **61**, 71 (1980).
7. R. Rapp, Acta Phys. Pol. B **42**, 2823 (2011).
8. H. van Hees, C. Gale, R. Rapp, Phys. Rev. C **84**, 054906 (2011).
9. G.J. Gounaris, J.J. Sakurai, Phys. Rev. Lett. **21**, 244 (1968).
10. N.M. Kroll, T.D. Lee, B. Zumino, Phys. Rev. **157**, 1376 (1967).
11. P.M. Hohler, R. Rapp, Phys. Lett. B **731**, 103 (2014).
12. R. Rapp, J. Wambach, Eur. Phys. J. A **6**, 415 (1999).
13. R. Rapp, J. Wambach, Adv. Nucl. Phys. **25**, 1 (2000).
14. T. Hatsuda, Y. Koike, S.-H. Lee, Nucl. Phys. B **394**, 221 (1993).
15. J.I. Kapusta, E.V. Shuryak, Phys. Rev. D **49**, 4694 (1994).
16. P.M. Hohler, R. Rapp, Ann. Phys. **368**, 70 (2016).
17. P.M. Hohler, R. Rapp, Phys. Rev. D **89**, 125013 (2014).
18. G. Aarts, C. Allton, S. Hands, B. Jäger, C. Praki, J.-I. Skullerud, Phys. Rev. D **92**, 014503 (2015).
19. NA60 Collaboration (H.J. Specht), AIP Conf. Proc. **1322**, 1 (2010).
20. CERES/NA45 Collaboration (D. Adamova *et al.*), Phys. Rev. Lett. **91**, 042301 (2003).
21. CERES/NA45 Collaboration (G. Agakichiev *et al.*), Eur. Phys. J. C **41**, 475 (2005).
22. STAR Collaboration (P. Huck), Nucl. Phys. A **931**, 659 (2014).
23. STAR Collaboration (L. Adamczyk *et al.*), Phys. Rev. C **92**, 024912 (2015).
24. R. Rapp, Adv. High Energy Phys. **2013**, 148253 (2013).
25. S. Endres, H. van Hees, J. Weil, M. Bleicher, Phys. Rev. C **91**, 054911 (2015).
26. S. Endres, H. van Hees, J. Weil, M. Bleicher, Phys. Rev. C **92**, 014911 (2015).
27. PHENIX Collaboration (A. Adare *et al.*), Phys. Rev. C **81**, 034911 (2010).
28. R. Rapp, H. van Hees, Phys. Lett. B **753**, 586 (2016).
29. PHENIX Collaboration (A. Adare *et al.*), Phys. Rev. C **93**, 014904 (2016).